PHYSICAL REVIEW B VOLUME 40, NUMBER 3 15 JULY 1989-II

Effects of the nearest neighbors and the alloy matrix on SiH stretching vibrations in the amorphous SiO_r:H ($0<r<2$) alloy system

D. V. Tsu, G. Lucovsky, and B. N. Davidson
Department of Physics and Department of Materials Science and Engineering, North Carolina State University, Raleigh, North Carolina 27695-8202

(Received 10 February 1989)

Hydrogenated silicon suboxides, SiO_r:H, for alloy range ($0<r<2$) have been deposited by remote plasma-enhanced chemical vapor deposition (remote PECVD) under conditions in which hydrogen is incorporated predominantly in monohydride or SiH bonding configurations. We have investigated both the SiH bond-stretching and bond-bending absorption bands by infrared (ir) absorption spectroscopy as a function of r, the alloy composition. In this paper, we have focused on the bond-stretching absorption bands, and have modeled the shape of the bond-stretching band as a function of the alloy composition. There are four distinct local environments for the SiH group in the suboxides; these can be written as HSi-$Si_{3-n}O_n$, for $n=0$–3. A sum of Gaussian functions, one for each environment, is used to synthesize the absorption in the SiH stretching band. The peak positions of these Gaussians are calculated by an induction model which includes both local and matrix (or alloy) effects; the amplitude weightings are determined from a random statistical model for the local bonding environments of the Si—O groups in the SiO_r alloy. We find that the frequency shifts caused by changes in the matrix, and associated with different values of r, are comparable to the shifts associated with the different local environments. The combination of these effects serves to diminish the discreteness of subband features in the absorption spectrum.

I. INTRODUCTION

There have been many studies of the vibrational properties of SiH bonding groups in amorphous silicon, a-Si:H,[1–3] amorphous suboxides of silicon, a-SiO_r:H,[4–7] and amorphous silicon dioxide, a-SiO_2:H.[7,8] In spite of these efforts, there has been no study to date that has systematically tracked the vibrational properties of the silicon monohydride (SiH) bonding group over the entire alloy range between a-Si and a-SiO_2. This derives in part from problems associated with sample preparation, in the context of being able to simultaneously change the O- to Si-atom ratio, while maintaining a sufficiently low hydrogen-atom incorporation to promote only SiH bonding groups and not the higher hydride groups such as silicon dihydride and polyhydride groups (SiH_2 and $(SiH_2)_n$, respectively). In addition, it is necessary to use a deposition process that at the same time precludes H-atom incorporation in SiOH groups. This paper addresses these questions of sample preparation by using a single deposition process, remote plasma-enhanced chemical vapor deposition (PECVD),[9] in which we are able to control simultaneously (1) r, the O- to Si-atom ratio and, hence, the degree of suboxide character; (2) the bonded-hydrogen concentration; and (3) the nature of the local-bonding groups into which hydrogen atoms are incorporated, e.g., SiH, SiH_2, SiOH, etc.[10–12] In particular, using the remote PECVD process, we show in this paper that we are able to produce films in which the hydrogen incorporation, as determined by ir spectroscopy, can be restricted predominantly to the SiH bonding configuration over the entire alloy range, $0<r<2$.

Extensive ir studies of SiH vibrations in silicon suboxides have been performed on suboxides whose [O]/[Si] ratio is less than about 1.0.[4–7] In these films, the SiH local-bonding configurations which predominate are the HSi-Si_3 and HSi-Si_2O configurations. Replacing one of the three nearest-neighbor Si atoms by the O atom results in three hydrogen-related ir absorption bands, one associated with a stretching mode (at 2100 cm^{-1}) and two with bending modes (at 790 and 640 cm^{-1}). The results of these studies showed that the double degeneracy of the SiH bending vibration in the HSi-Si_3 configuration is removed by the decrease in symmetry promoted by the presence of oxygen in the HSi-Si_2O configuration. In the present paper, we extend the vibrational study of the SiH group to suboxides with larger O- to Si-atom ratios, up to 2.0, in which there are, in addition, local-bonding groups with two and three oxygen nearest neighbors. We focus on the detailed shape of the monohydride stretching band, and the changes that occur as the alloy composition is varied.

The region of the ir spectrum below about 1200 cm^{-1} contains both the SiO absorption bands and the SiH bond-bending bands. The position of the principal absorption, i.e., the SiO bond-stretching band, is sensitive to the value of the [O]/[Si] ratio, and has been used to determine the alloy composition.[7,13] The multiplicity of features in the SiH bending regime of the ir spectrum is used to confirm that the hydrogen is incorporated mostly in the monohydride bonding configuration. In addition, because the SiH bending mode in the HSi—O_3 is doubly degenerate due to the local symmetry, only one bending absorption band is expected. This feature has enabled us to further confirm some of the stretching-mode assignments. A more detailed discussion of the bending modes will be presented in a future publication.[14]

In this paper, we develop a model which accounts for the change in shape of the SiH stretching band with alloy composition. This model includes the effects of the nearest-neighbor environment or local-bonding environments, as well as those of the alloy network. A model that has been shown to be useful for the analysis of the changes to the stretching band frequency as a function of the nearest neighbor chemical-bonding environments is based on a chemical-induction effect.[15] The basis for this model is an empirical scaling relationship, relating the changes in the SiH stretching frequency to changes in the electronegativity of the local environment of the SiH group caused by the replacement of a less electronegative species, the Si atoms, with the more electronegative O atoms. In its simplest form, this model predicts that the SiH stretching band in a SiO_r alloy can be constructed from four distinct subbands, one for each of the four possible distinct local environments of the SiH group. These groups can be written as $HSi—Si_{3-n}O_n$, for $n=0$ to 3, and the expected frequencies, based solely on the four nearest-neighbor environments, are 2000, 2100, 2195, and 2265 cm^{-1}, respectively, for $n=0$, 1, 2, and 3.[5-7] Experimentally, we show, however, that this local model cannot account for all of the observed changes in this band with alloy composition. To this end, we have found it necessary to extend the induction model to include, in addition to the effects of the local bonding, the chemical-induction effects of more distinct neighbors as they reflect the average alloy composition.[16]

Section II of this paper discusses sample preparation by the remote PECVD process. Section III presents the ir data and Sec. IV includes the analysis of this data. Section V is a summary of our results, including a discussion of the applicability of our experimental and analytical approaches to SiH vibrations in other related alloy systems such as $a\text{-}SiN_r$:H and $a\text{-}Si_xO_yN_z$:H.

II. SAMPLE PREPARATION

All of the thin films produced in this study were deposited in a combined deposition-analysis system that has been described in detail in previous publications.[17,18] Figure 1 shows a schematic of a "section" of the chamber containing the plasma tube and the first gas-dispersal ring. The chamber is made of 2-in.-o.d. stainless-steel (SS) tubing, and contains five analyzing stations and two gas-dispersal rings. Each analyzing station consists of three ports: one port for mass spectrometry (MS) and two for optical studies, primarily optical-emission spectroscopy (OES). The first two stations and the first gas-dispersal ring are shown in Fig. 1. The silane mixture (10 vol % SiH_4, 90 vol % Ar) is introduced into the chamber through the gas-dispersal ring at a flow rate of 10 standard cm^3/min (sccm). The O_2-He mixture, delivered at a flow rate of 100 sccm, flows through the plasma tube, past the plasma bias plates, and then into the chamber region. The relative concentration of O_2 in He was varied between 0 and 1.0% by varying the relative flow rates of a 1.0% O_2-in-He source gas, and a pure-He source gas. The plasma tube consists of 32-mm-o.d. vitreous silica tubing approximately 10 in. long, and the rf power for this study was set at 29±1 W. The substrate-sample heater block assembly is movable, and can be positioned anywhere along the length of the chamber. For this work, it was positioned at station 2, which is 7 in. downstream from the end of the plasma tube. With the exception of film 40, whose ir spectrum is shown in Fig. 2, all of the other films in this study were deposited at a sample-block temperature (T_B) of 225 °C. In addition, the sample block was biased −125 V with respect to ground. Under this substrate temperature and bias condition, the dihydride component in the resulting a-Si:H (Ref. 12) and suboxide films is minimized. Film 40 was deposited under conditions which promote dihydride incorporation, i.e., low substrate temperature ($T_B = 125\,°C$) and no applied electrical bias to the sample probe; in other words, the sample probe was electrically floating. Finally, the pressure is measured with a Baratron and maintained at 300 mTorr using a downstream throttle controller. The process gases are pumped by a rotary vain pump with a pumping speed of 55 ft^3/min (CFM).

The plasma bias plates consist of four rectangular Al plates arranged in a *boxlike* configuration coaxial with

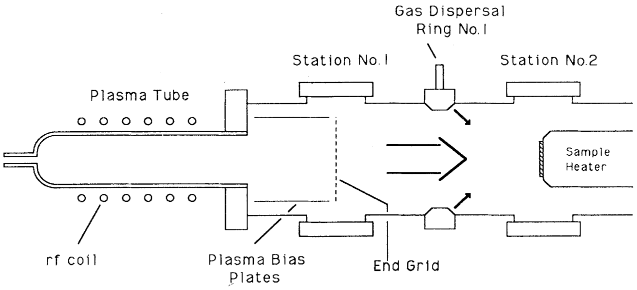

FIG. 1. Remote PECVD deposition-analysis chamber.

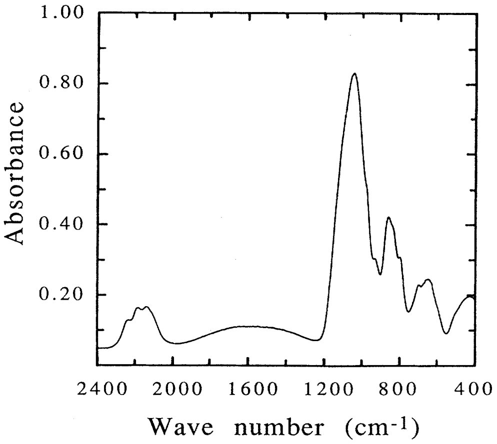

FIG. 2. ir absorbance spectrum of film 40. This film was deposited under conditions which promote the incorporation of SiH_2 bonding groups.

the chamber, and a circular no. 10 mesh SS screen grid capping the end of this box. The plates and the grid are supported by Teflon and can be biased independently. In this study, only one condition was varied: the relative O_2 concentration in He, between 0 and 1.0%, and not the plasma bias. We showed in a recent publication[18] that the bias state of the end grid, either *electrically floating or grounded,* was critical in being able to deposite suboxides. The four Al plates were electrically floating during the entire study. When the end grid is *grounded,* the plasma afterglow, as can be observed from the view port of station 1, extends downstream from the grid. On the other hand, when the grid is allowed to *float,* the plasma glow is observed to stop at the grid and the afterglow does *not* extend downstream into the chamber region. Under the grounded condition, silicon suboxides can be deposited, while under the floating condition silicon dioxide (SiO_2) is deposited for *all* O_2 concentrations investigated, between 0.1 and 1.0% in He. Only the SiO_2 deposition rate changed in the latter case. To deposit the suboxides for this study, the end grid was therefore always used in the grounded state.

III. THE ir DATA

The thin films produced in the apparatus described above were deposited onto crystalline Si substrates (10–100 Ω cm) and examined with an infrared (ir) spectrophotometer, Perkin-Elmer model PE983. Figure 2 shows the ir absorbance spectrum of film 40. The O_2 concentration in He used to produce this film is 0.5%. As discussed in the preceding section, this film was deposited under temperature and sample bias conditions which promote the incorporation of silicon dihydride groups. This spectrum is included in order to provide a basis for evaluating the extent to which polyhydride groups have been eliminated in other samples. Evidence for these polyhydride groups is found in both the SiH bond-stretching and bond-bending regions of the ir spectrum.

The SiH bond-stretching band, between 2300 and 2000 cm^{-1}, shows four features, including the three distinct peaks at 2240, 2190, and 2145 cm^{-1}, as well as a shoulder at about 2110 cm^{-1}. As will be discussed in the following section, these features are a result of a change in the SiH stretching frequency due to changes in the atomic composition of the local environment of the SiH group, i.e., the distribution of the Si and O atoms on the three backbonds of the Si atom of the SiH group. Because each subband represents a particular local environment, they can in principle be used to identify the precise environment. We will show, however, that the effective electronegativity of the Si atom of the Si-H group, and thus the vibrational frequency, can be affected not only by changes in the relative number of O and Si atoms occupying the three nearest-neighbor sites of the SiH group, but also by changes in the [O]/[Si] ratio of the suboxide matrix itself; i.e., by the average properties of more distant neighbors.[16] In addition, the same mechanisms apply to the frequencies of the SiH_2 group as well. These effects then combine, with the result being a multiplicity of possible frequencies, with absorption features from the SiH group overlapping with the features from the SiH_2 group. This makes the identification of the four features in sample 40 ambiguous.

However, the issue of dihydride incorporation can be resolved with the help of the SiH bond-bending region of the ir spectrum. The principal absorption feature at 1045 cm^{-1} is due to the SiO bond-stretching vibration. The distinct and sharp features in the spectrum below about 1000 cm^{-1} are associated with SiH bond-bending-type modes. The SiO bond-bending absorption band at about 810 cm^{-1} may be buried under the SiH bands and the absorption band at roughly 450 cm^{-1} is due to SiO rocking vibrations. The richness of the spectrum in this region reflects changes in the symmetry of the bending mode as the relative number of O- and Si-atom nearest-neighbor changes. Specifically, when the SiH group has either three Si-atom or three O-atom nearest neighbors, the bending mode is doubly degenerate; any combination of Si and O atoms lifts the degeneracy resulting in two different bands for each of the two mixed second-neighbor configurations, i.e., for $HSi\text{-}Si_{3-n}O_n$ with $n=1$ or 2. We point out, however, the existence of two spectral features, one a shoulder at 976 cm^{-1} on the low-frequency side of the SiO stretching band, and the other a distinct peak at 935 cm^{-1}, which we propose are associated with SiH bending modes of a $H_2Si\text{-}O_2$ group. Evidence for this association derives from two sources. First, a deuteration experiment, where SiH_4 is replaced with SiD_4 in the deposition process,[10,14] has shown that these features are removed from the ir spectrum and are thus shown to be hydrogen related. Second, the difference in frequency of about 40 cm^{-1} between these two features is about the same as the difference in frequency between the 890-cm^{-1} scissors bending mode and the 845-cm^{-1} wagging mode of polymerized dihydride in *a*-Si:H.[3] The induction mechanism which increases the SiH bond-stretching frequency from 2000 cm^{-1} in *a*-Si:H to about 2265 cm^{-1} in *a*-SiO_2 also leads to an increase in frequency of these bond-bending modes.

As we have stated above, it is the intention of this work to investigate the monohydride group in the suboxides. We have shown in the above discussion that, although both the bond-stretching and bond-bending regimes of the ir spectrum can be used as spectroscopic tools for the investigation of dihydride bonding groups, only in the bending regime can the spectrum be unambiguously interpreted; we believe that the (976-, 935-) cm^{-1} "doublet" indicates the presence of dihydride bonding groups. It is therefore expected that the (976-, 935-) cm^{-1} features, apparent in the spectrum of film 40, should not appear in the bond-bending regime of films deposited under the conditions which minimize the incorporation of dihydride groups. The ir absorbance spectra of the SiH bond-stretching regime and the bond-bending regime for suboxide films deposited under these conditions are shown in Figs. 3 and 4, respectively. The (976-, 935-) cm^{-1} features associated with dihydride bonding groups are in fact not observed in any of the spectra in Fig. 4. A summary of the O_2-flow conditions and various film properties for these 12 films is given in Table I, and this then allows us to analyze the bond-stretching features shown

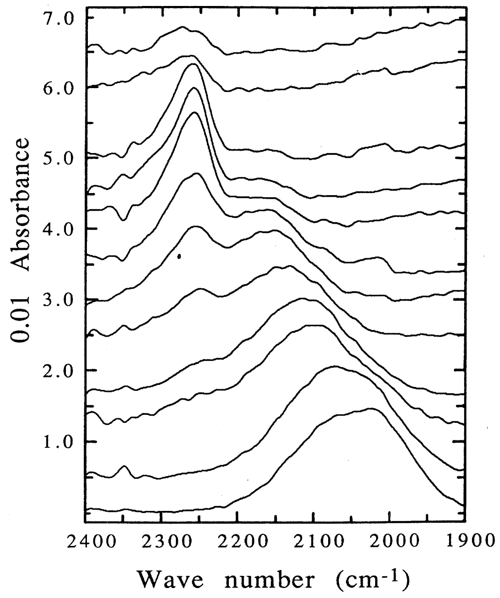

FIG. 3. ir absorbance spectra in the SiH bond-stretching regime of films deposited under conditions which minimize the incorporation of the dihydride groups. (See Table I for a description of these films.)

in Fig. 3 in terms of only monohydride (SiH) -type vibrations. The thickness of these films, used to calculate the absorption constant for the SiO stretching band, was determined with a Dektak profilometer. In most cases, a sharp step could be achieved by protecting the thin film with beeswax and etching an edge region with concentrated HF acid. For the suboxides deposited using oxygen concentrations below 0.4%, however, the etching technique did not work and we had to rely on physically masking the substrate during deposition to create the step.

The spectra in Figs. 3 and 4 are presented in the same order as the listing in Table I, i.e., the spectrum of the film deposited under the highest O_2 concentration (film 57, $[O_2]=0.90\%$) is the topmost spectrum, while that under the lowest O_2 concentration (film 53, $[O_2]=0.10\%$) is the bottom-most spectrum. The stretching-band regime (Fig. 3) shows the existence of two distinct subbands: a relatively narrow band [full width at half maximum (FWHM) ≈ 50 cm^{-1}], whose peak position is roughly at

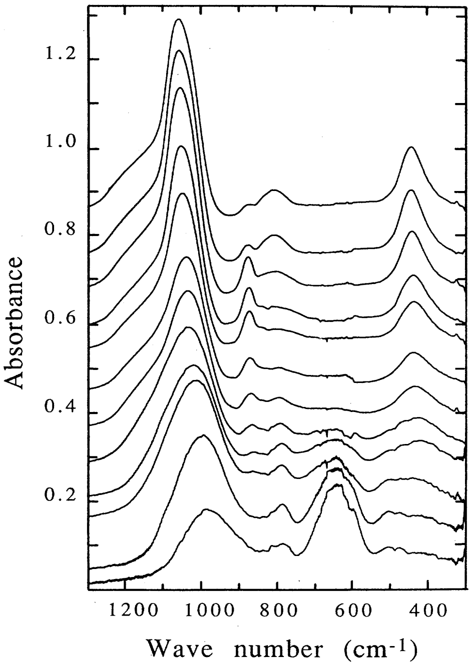

FIG. 4. ir absorbance spectra in the SiH bond-bending regime of the same films as in Fig. 3. Some of the spectra in this figure have been multiplied by a constant to facilitate plotting on the same scale: (1) film 57, ×0.8; (2) film 56, ×0.9; (8) film 47, ×1.5; (9) film 51, ×1.5; (10) film 62, ×2.0; (11) film 52, ×3.0; and (12) film 53, ×4.0. (See Table I for a description of these films.)

TABLE I. Deposition and various film parameters of the suboxides deposited under conditions which minimize the incorporation of SiH_2 groups. The ir spectra of these films are shown in Figs. 3 and 4.

Film no.	O_2 in He (%)	thickness (Å)±100	SiO stretching mode ω (cm^{-1})	SiO stretching mode α (10^3 cm^{-1})	r, [O]/[Si]
57	0.90	5600	1062	22.2	1.94
56	0.80	4700	1061	25.4	1.92
58	0.60	4000	1058	26.1	1.86
55	0.55	3200	1058	28.7	1.86
59	0.50	3500	1054	22.5	1.78
61	0.45	3500	1042	18.6	1.54
49	0.45	3700	1041	17.5	1.52
47	0.40	2300	1039	18.0	1.48
51	0.35	2200	1024	17.0	1.18
62	0.30	2900	1020	10.0	1.10
52	0.20	2600	998	5.9	0.66
53	0.10	2000	985	3.6	0.40

2265 cm^{-1} and shows a slight frequency dependence on the O_2- flow rate, varying between about 2270 and 2260 cm^{-1}, and a relatively broad band, whose peak position shows a large frequency dependence, varying between about 2200 and 2000 cm^{-1}. In general, the higher-frequency peaks are associated with the higher O_2 flow rates. The higher O_2 flow rates in turn result in films with higher concentrations of bonded oxygen, i.e., in films whose [O]/[Si] ratio approaches 2.0. This aspect of the data and the data analysis is discussed below.

The spectrum of film 57 in the range between 1300 and 300 cm^{-1} shown in Fig. 4 shows the three principal Si-O absorption bands of SiO_2 and one hydrogen-related band: the SiO bands at 1062, 813, and 447 cm^{-1} are the stretching, bending, and the rocking bands, respectively.[19] The additional hydrogen-related feature is at about 876 cm^{-1}. The local environment of the Si atoms in this film is expected to be nearly identical with the Si atoms in SiO_2, with the exception of those atoms to which hydrogen is bonded, i.e., each Si atom has either four O-atom neighbors or one H atom and three O-atom neighbors. We then associate the 876-cm^{-1} band with the hydrogen bending motion in the HSi-O_3 configuration. This assignment is in agreement with those reported previously.[5,7] As the O_2 concentration decreases, the character of the three Si—O bands is changed. In particular, there are three modifications to the Si—O bond-stretching band that are consistent with the expected changes resulting from a decrease in the [O]/[Si] ratio r from 2.0 to 0:[7,13,19] (i) the position of the spectral peak decreases, (ii) the characteristic shoulder on the high-frequency side of the band disappears, and (iii) the full width at half maximum (FWHM) absorbance increases. Pai *et al.*[5] measured r for suboxides with the electron microprobe technique and found that it scaled in an approximately linear fashion with the peak frequency of the Si—O bond-stretching absorption band. We use this secondary calibration technique to determine r for the suboxides deposited in this study. The expression

$$\nu=965+50r \ \text{cm}^{-1} \tag{1}$$

is used to find r from the experimentally determined position of the peak frequency ν. The value 965 cm^{-1} in Eq. (1) is approximately the SiO stretching frequency of an O atom in an *a*-Si:H network[7] and the slope of 50 cm^{-1} ensures that the frequency is 1065 cm^{-1} for the SiO_2 end point. This frequency can vary between about 1080 cm^{-1} for thermally grown SiO_2 (Ref. 20) to about 1055 cm^{-1} for SiO_2 deposited by the low-temperature PECVD techniques. The frequency at the *a*-Si:H endpoint can also vary, between about 940 and 980 cm^{-1}, depending on the bonded hydrogen concentration.[7] The ambiguity of the end points is a principal source of error in the determination of r by this technique, but the error is less than about 20%. Determining the value of r to within this error, however, is sufficient for this study. The Si—O stretching frequency for each spectrum shown in Fig. 4 is listed in Table I along with the value of r derived from Eq. (1). We conclude that the bonded oxygen concentration can be directly controlled by varying the O_2 concentration in He.

The changes that occur in the SiH stretching band shown in Fig. 3 are then correlated with a decrease in the bonded-oxygen concentration and the corresponding changes to the SiH bending band are shown in Fig. 4. The bottom-most spectrum in Fig. 4, film 53, shows two absorption bands related to the SiH bending vibration: these are at 635 and 790 cm^{-1}. Lucovsky *et al.*[7] have shown that these bands occur when the SiH group has one O-atom nearest neighbor, i.e., for the HSi-OSi_2 configuration. In particular, it was shown that the 790 cm^{-1} band is related to the a SiH bending vibration in which the motion is in the plane defined by the H-Si-O-Si unit and which couples to the SiO bending vibration for the cis orientation of this unit. In the cis orientation, the H and O atoms are on the *same side* of a line drawn through the two Si atoms. The 635-cm^{-1} band is associated with SiH bending modes in the trans orientation and to hydrogen motions perpendicular to the plane defined by the three H-Si-O atoms. In addition, the 635-cm^{-1} band also occurs for each bending vibration of the HSi-Si_3 configuration.[1-3,7]

Figure 4 shows that as the oxygen concentration increases in the film, both the 635- and 790-cm^{-1} bands disappear and are replaced by the 876-cm^{-1} band, which itself disappears as r approaches 2.0. In the following section, we show that these changes, and the corresponding changes in the SiH stretching band as shown in Fig. 3, are a direct result of an increase in the probability that more than one of the three nearest-neighbor sites of the SiH group are occupied by an oxygen atom. For [O]/[Si] ratios greater than about 1.9, the probability that three O atoms occupy these sites approaches unity, and the 876-cm^{-1} band is associated with the hydrogen bending vibration of this configuration; this is discussed in more detail in the next section.

IV. DATA REDUCTION AND ANALYSIS

A. The 2265- and 876-cm^{-1} bands

A comparison of Figs. 3 and 4 with Table I reveals that when the relative O_2 concentration in He is between 1.0% and about 0.6%, there are two distinct absorption bands in addition to the three SiO bands, one at about 2265 cm^{-1} and the other at 876 cm^{-1}. These are assigned to the bond-stretching and bond-bending vibrations of the SiH group, respectively, in the three-O, i.e., the HSi-O_3, configuration.[5] The experimental evidence for this conclusion is based on a comparison of the peak positions of these absorption bands in films deposited using both hydrogenated and deuterated silane (SiH_4 and SiD_4), and on a direct comparison of the absorption amplitudes of the 2265- and 876-cm^{-1} absorption bands. In addition, we present two arguments which further support the assignment to the HSi-O_3 configuration: the first is based on symmetry considerations alone, and the second is based on the observation that these features are seen only in the spectra of films having an [O]/[Si] ratio greater than about 1.9.

We have shown in a previous publication[10] a comparison of the ir spectra of suboxides deposited from both SiH_4 and SiD_4 source gases. In the hydrogenated sample, the ir spectrum contained both the 2265- and 876-cm^{-1} bands that we have assigned to the SiH stretching and bending modes, respectively, in the HSi-O$_3$ configuration. In the deuterated sample, these bands were absent but were replaced by two other absorption bands at 1638 and 620 cm^{-1}, which we associate with the SiD stretching and bending modes, respectively, in the DSi-O$_3$ configuration. The ratio of the bond-stretching frequencies between the two bond-stretching vibrations SiH and SiD of about 1.38 is in accord with a simple calculation based on an isotopic mass substitution of D for H. The ratio of the bending-mode frequencies (about 1.40) is higher than what would be expected (less than about 1.2) for similar modeling. This discrepancy will be discussed in a future publication,[14] where we show that this enhanced ratio is a result of mode-coupling effects involving a Si—O vibration, which shift the SiH bending mode to a higher frequency, but which do not effect the frequency of the SiD bending mode.

A plot of the absorption constant at 2265 cm^{-1} versus the absorption at 876 cm^{-1}, corrected for the underlying shoulder of the Si—O bending band, displays a linear relationship demonstrating that these two absorption bands are due to vibrations of the same local-bonding arrangement. The result of this comparison is shown in Fig. 5. Only those films in which the 2265-cm^{-1} "subband" clearly dominated the SiH stretching band were used in this comparison, ensuring that only effects due to the three-O environment (and not the two-O environment) were considered. The line is a linear least-squares fit of the data; the value of the fit parameter ($r^2=0.90$) confirms the association between the two bands. The absorption constant of this bond-bending mode is about 4 times larger than that of the associated bond-stretching mode. This is approximately the same factor that is observed for the corresponding band strengths in a-Si:H.[1–3] This means that the same effective charge mechanisms for the two modes most likely prevail in the oxides, and that these mechanisms are not modified by the induction effects which promote significant shifts in the respective frequencies.

We have shown above that the 2265- and 876-cm^{-1} bands are associated with bonded hydrogen in the *same* bonding configuration. The band multiplicity, i.e., one stretching- and one bending-type vibration, is in accord with the C_{3v} symmetry of the HSi-O$_3$ configuration. This is the same local symmetry for a SiH vibration in a-Si:H, where the bonding configuration can be written as HS-Si$_3$. Additional evidence for this assignment is based on the fact that the three Si—O vibrations, at approximately 1062, 813, and 447 cm^{-1}, which are associated with stoichiometric SiO$_2$, are also observed in these same films. These three characteristic Si—O absorption bands can occur only in films where the Si atoms are surrounded predominantly by four O atoms.[19] We show in the following section that the probability the HSi-O$_3$ configuration occurs approaches unity as the [O]/[Si] ratio exceeds about 1.9. For these concentrations, and for monohydride hydrogen incorporation, those Si atoms to which the H atoms are bonded must then have three oxygen neighbors.

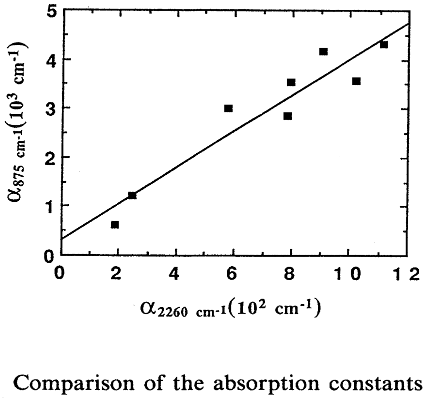

FIG. 5. Comparison of the absorption constants at 875 and 2265 cm^{-1}. These bands are due to the SiH bond-bending and stretching vibrations, respectively.

B. SiH stretching-band-shape dependence on the [O]/[Si] ratio

In the previous section, we showed that when the SiH (or D) group has three oxygen nearest neighbors, the shapes of both the stretching and bending bands are relatively simple, i.e., the stretching and bending bands can approximately be represented as Gaussian functions whose peak positions are at about 2265 cm^{-1} (1638 cm^{-1} for SiD) and 875 cm^{-1} (620 cm^{-1} for SiD), respectively. The same could be said of films at the other end in the alloy composition, i.e., in a-Si:H films, where the SiH group has three silicon neighbors. In this case the (approximately) Gaussian functions representing the SiH stretching and bending absorption bands have peak positions of about 1985 and 635 cm^{-1},[1–3,11] respectively. As Fig. 3 shows, films with [O]/[Si] ratios between a-SiO$_{1.9}$:H and a-Si:H, have absorption bands that cannot be represented by a single Gaussian function, i.e., the spectra show more than one feature. We now proceed to develop a quantitative model which can account for this increase in structure in the shape of the SiH stretching band.

There are two main assumptions in our model: (i) the nearest-neighbor environment of the SiH group is determined by the statistics of Si—O bonding arrangements in a random covalent-network-bonding model;[21] and (ii) the SiH stretching frequency is determined by an induction model involving an empirical scaling relationship which is based on changes in the local electronegativity.[15] The first part of the model gives the probability that a SiH group will have a certain number of oxygen and silicon nearest neighbors as the [O]/[Si] ratio r varies between 0 and 2 for SiO$_r$. For this we use the same representation of suboxides first put forward by Philipp.[21] In this representation, the suboxide is composed of Si-centered tetrahedra of the form Si-Si$_{4-m}$O$_m$, for $m=0$ to 4; simple statistics determines the weighting factors for each value of m. In this paper, we extend Philipp's model to include the effects of hydrogen bonded in SiH groups. We show below that in the second part of the model the SiH frequency depends on the local electronegativity, and this in turn depends most strongly on the relative number of oxygen and silicon nearest-neighbor atoms, but, in addition, is modified by the effects of more distant neighbors, the so-called remote induction effect.[16] The four distinct environments, written as $\mathrm{HSi\text{-}Si}_{3-n}\mathrm{O}_n$, for $n=0$ to 3, result in four distinct SiH stretching subbands.

These two features of the model provide a quantitative means for obtaining amplitudes and positions of the individual SiH absorption subbands for each alloy composition. This then provides a basis from which the SiH absorption band can be synthesized for each r, or [O]/[Si] ratio. Because there is no theory for the shapes of the individual subbands, we simply assume that the noncrystalline nature of the material promotes subbands which can be approximated by Gaussian functions.[22] We use the spectra shown in Fig. 3 as a guide to choosing the appropriate widths to use for these Gaussian subbands.

We begin with the Philipp model, which applies to silicon suboxides containing no hydrogen. In this model, the probability that one or more of the four nearest-neighbor sites of a silicon atom is occupied by O atoms and/or Si atoms is determined. If u is the probability that one of the four available sites is occupied by an O atom, and v is the probability that it is occupied by a Si atom, the probability of finding the four sites occupied by either O or Si atoms is given by

$$P(u,v)=(u+v)^4 , \tag{2}$$

which, by definition, must equal 1, because

$$v=1-u . \tag{3}$$

Expansion of Eq. (2) yields

$$P(u,v)=u^4+4u^3v+6u^2v^2+4uv^3+v^4 . \tag{4}$$

The first term is the probability that the Si atom has four oxygen nearest neighbors, the second term is the probability that the four neighbors consist of three O atoms and one Si atom, etc. When $u=1$, the four neighbors are all oxygen atoms, and when $v=1$, they are all silicon atoms. The resulting structural building blocks for these alloy end points are those found in SiO_2 and a-Si, respectively. It is therefore possible to express Eq. (2) in terms of the [O]/[Si] ratio r found in the SiO_r suboxide expression if we write

$$u=r/2 . \tag{5}$$

We now consider how the probability function is affected when hydrogen is allowed to be one (but not more than one) of the four nearest neighbors. If w is the probability that one of the four sites is occupied by a hydrogen atom, then

$$P(u,v,w)=(u+v)^4+4w(u+v)^3 , \tag{6}$$

which must also equal 1. The interpretation of the quartic term is the same as in Eq. (2), but because of the hydrogen, Eq. (3) does not strictly hold for Eq. (6). Expansion of the cubic term gives the probability that one of the four nearest neighbors is hydrogen and the other three are silicon and/or oxygen atoms. A relationship between u, v, and w which satisfies the $P(u,v,w)=1$ condition can be obtained by expressing w in terms of u and v:

$$w=a(u+v) , \tag{7}$$

where a is the percent hydrogen in the film. Equations (6) and (7), with the $P=1$ condition, give

$$v=(1+4a)^{-1/4}-u . \tag{8}$$

For small hydrogen concentrations, i.e., small a, Eq. (8) can be expanded to give

$$v=1-u-a+\tfrac{5}{2}a^2 . \tag{9}$$

Thus when [H] is small, i.e., below about 10 at. %, the hydrogen makes a small perturbation of the statistical distribution of Si and O atoms. It is therefore valid to use Eq. (3) and the cubic term in Eq. (6) to obtain the relative statistical distribution of the three nearest neighbors of the SiH group in suboxides, $P(\mathrm{SiH})$:

$$\begin{aligned} P(\mathrm{SiH}) &= (u+v)^3 \\ &= u^3+3u^2(1-u)+3u(1-u)^2+(1-u)^3 \\ &= P_3(u)+P_2(u)+P_1(u)+P_0(u) \\ &= \sum_n P_n(u) , \end{aligned} \tag{10}$$

where $P_n(u)$ is the relative probability the SiH group has n oxygen nearest neighbors. With the use of Eq. (5), each term in Eq. (10) is plotted in Fig. 6 as a function of the alloy composition.

The second part of the model concerns the shifts in frequency of the SiH stretching vibration as the local environment of the SiH group changes with alloy composition. In previous work,[11] we confirmed that the increase in the SiH stretching frequency in remote PECVD a-Si:H films as the hydrogen concentration increases could be accounted for by an empirical scaling relationship involving changes in the local electronegativity of the surrounding medium of the SiH group.[16] These changes are

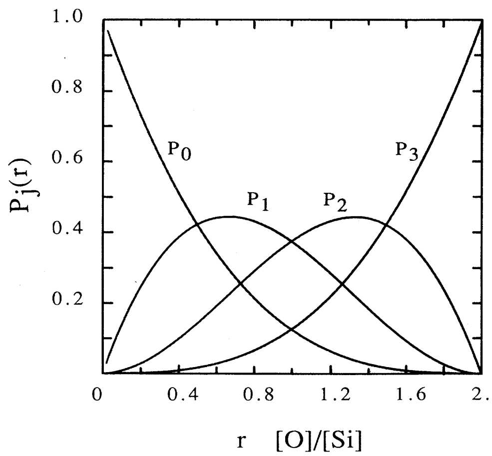

FIG. 6. The relative probability $P_j(r)$ that the SiH group has j oxygen nearest neighbors vs the [O]/[Si] ratio r.

caused by the incorporation of a more electronegative atomic species (other hydrogen atoms) in the silicon network and has the net effect of transferring charge away from the Si atoms of the SiH bonds. The end result is an increase in frequency of the SiH stretching vibration; this model is known as the chemical-induction model,[15] and includes the so-called remote induction effects that have been shown to apply in both molecules[16] and in amorphous materials.[15]

We found that the hydrogen in *a*-Si:H films produced by the remote PECVD technique is bonded predominantly in the monohydride (SiH) configuration for substrate temperatures above about 100 °C (Refs. 11 and 12) and, thus, changes in the SiH frequency could be studied without the complicating effects involving the growth of a dihydride (SiH_2) band. For films containing the smallest amount of hydrogen, just above the ir detection limit of about 1 at. %, the SiH frequency is 1985 cm^{-1}. As the hydrogen concentration increased, the local electronegativity increased and the frequency increased linearly to 2010 cm^{-1} at a concentration of 18 at. %. These systematic changes in the SiH bond-stretching frequency could be explained in the context of the remote neighbor induction mechanism.[15,16] The same formalism is used in the present work to account for changes in the SiH stretching frequency with changes in the SiO_r alloy composition; the greater electronegativity of oxygen as compared to silicon (or to hydrogen) draws charge away from the Si atom of the SiH bond, leading to increases in the stretching frequency.

The induction model[15] assumes that the SiH vibrational frequency is directly proportional to the average electronegativity of the near-neighbor environment, i.e.,

$$\nu=\nu_0+b\sum X_A \;, \tag{11}$$

where the constants ν_0 and b are determined empirically, X_A is the stability-ratio electronegativity (SRX),[23] and the sum is over the three neighbors of the SiH group. The constants are determined by calculating X_A for the SiH group in *a*-Si, Si_3N_4, and SiO_2 and using the experimentally determined SiH frequencies in these materials, 1985, 2180, and 2260 cm^{-1}, respectively. In calculating X_A, we perform a geometric average[16] of the SRX's of both the nearest neighbor, X_{nn}, and the next-nearest neighbor, X_{nnn}, i.e.,

$$X_A=[X_{nn}(X_{nnn})^k]^{1/(1+k)} \;, \tag{12}$$

where k is the number of next-nearest-neighbor (nnn) sites (one for O atoms and two for N atoms). For the nitride and oxide, N and O atoms, respectively, are taken to be the nearest neighbors (nn) and the next-nearest neighbors (nnn) the effective media of Si_3N_4 and SiO_2. The SRX's for the atomic species are the following: $X_{Si}=2.62$, $X_H=3.55$, $X_O=5.21$, and $X_N=4.49$. The SRX's of the effective media are determined by geometrically averaging the SRX's of the atomic constituents,[15,16,23] i.e.,

$$X_{SiO_2}=[X_{Si}^1X_O^2]^{1/3}=4.14 \tag{13}$$

and

$$X_{Si_3N_4}=[X_{Si}^3X_N^4]^{1/7}=3.56 \;. \tag{14}$$

The SRX for the effective medium of *a*-Si is the same as for atomic Si, i.e., $X_{a\text{-}Si}=X_{Si}$. X_A is calculated by Eq. (12) and multiplied by 3 (to obtain $\sum X_A$) for each material and is plotted in Fig. 7 with respect to the SiH stretching frequencies in those materials. The line represents a linear least-squares fit of the data, which therefore supplies the constants in Eq. (11). Equation (11) becomes

$$\nu=1630+46\sum X_A \pm 12\ cm^{-1} \;. \tag{15}$$

The constants ν_0 and b derived here for the solid materials are slightly different from the values (1740.7 and 34.7) found by Lucovsky[15] for the molecular compounds. Differences in the mode mass for the SiH group in the solids and in the gaseous molecules may account for these differences. To calculate the SRX of the effective medium in the suboxides, we carry out the same geometric averaging procedure, i.e.,

$$X_{SiO_r}=[X_{Si}X_O^r]^{1/(1+r)} \;, \tag{16}$$

where r varies between 0 and 2. The nearest neighbors are taken to be either Si or O atoms and the next-nearest neighbors the effective medium. X_A therefore depends on whether Si or O is the nearest neighbor. In case (a), where oxygen is the nearest neighbor, X_A becomes

$$X_A(a)=[X_OX_{SiO_r}]^{1/2} \;, \tag{17}$$

and in case (b), a silicon nearest neighbor yields

$$X_A(b)=[X_{Si}(X_{SiO_r})^3]^{1/4} \;. \tag{18}$$

There are thus four possible forms of $\sum X_A$, depending on the number n of oxygen nearest neighbors:

$$\sum X_A(n)=nX_A(a)+(3-n)X_A(b) \;, \tag{19}$$

where $n=0$, 1, 2, or 3. A schematic representation of the two-O ($n=2$) environment is shown in Fig. 8. Equations (15) and (19) are now used to determine the SiH stretching frequency for each of the four possible outcomes as a function of the [O]/[Si] ratio r. The results are plotted in Fig. 9. This figure shows that for any particular value of

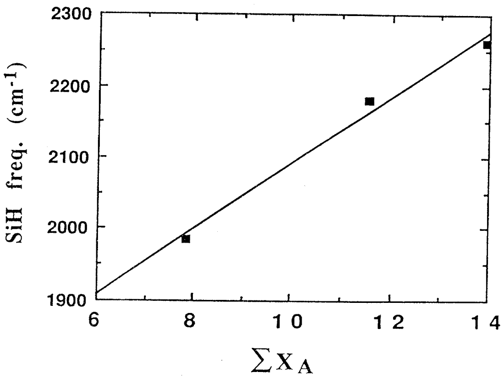

FIG. 7. SiH stretching frequency vs $\sum X_A$.

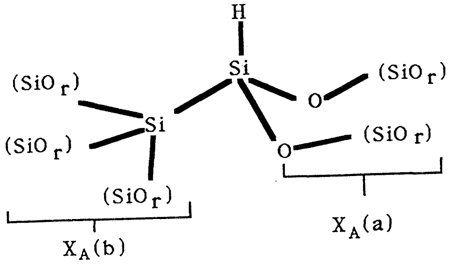

FIG. 8. Schematic representation of the HSi-O$_2$Si configuration.

r four distinct bands, separated by about 50 cm^{-1}, are expected. Moreover, the position of each band depends on the [O]/[Si] ratio of the host network. We found that changes in the effective electronegativity in a-Si:H with the introduction of hydrogen[11] lead to an increase in the SiH stretching frequency by as much as 25 cm^{-1}. This increase in frequency can be more than a factor of 10 greater in films containing oxygen because of the greater electronegativity of oxygen.

To synthesize the expected shape of the entire SiH stretching band, a sum over the subbands expected from each local environment is performed:

$$F(\nu,r)=\sum_{j=0}^{3} P_j(r)G(\nu_j(r),H_j) \ , \tag{20}$$

where the sum is over the different local environments, ν is the vibrational frequency, r the [O]/[Si] ratio, $P_j(r)$ the statistical amplitudes, and the normalized Gaussian function G is given by

$$G(\nu_j(r),H_j) = \left[\frac{2\ln 4}{\pi H_j^2}\right]^{1/2} \exp\left[\frac{-2\ln 4[\nu-\nu_j(r)]^2}{H_j^2}\right] \ , \tag{21}$$

which is written in terms of H_j, the full width at half maximum (FWHM) absorption. For a particular value of r, the amplitudes $P_j(r)$ and the frequencies $\nu_j(r)$ are determined from Figs. 6 and 9, respectively. To obtain the Gaussian widths, we must turn to the experimental spectra shown in Fig. 3. Unfortunately, as this figure indicates, it is possible to determine the width of only one of the subbands; the 2265-cm^{-1} subband for the HSi-O$_3$ configuration near the a-SiO$_2$ end point has a full width of roughly 50 cm^{-1}. On the other hand, ir studies of the opposite (a-Si:H) endpoint[11] have shown that the FWHM of the stretching band varies between about 65 cm^{-1} for low hydrogen concentrations (<1 at. %) and about 110 cm^{-1} for high concentrations (>18 at. %). Because the widths of the subbands are expected to fall within these values, we choose a width of 80 cm^{-1} for the three Gaussians representing the $j=0$, 1, and 2 subbands and a width of 50 cm^{-1} for the $j=3$ subband. Except for the experimentally determined value of 50 cm^{-1}, the choice of 80 cm^{-1} is more or less arbitrary. It can be shown, however, that as long as a value greater than about 60 cm^{-1} is used, no qualitative differences in the synthesized spectra occur. Values below 60 cm^{-1} would result in easily identifiable subbands, which, as Fig. 3 shows, do not occur.

The results of the Gaussian synthesis, Eq. (20), for a range of suboxide alloys is shown in Fig. 10. In this figure, r decreases from 1.80 for the top spectrum to 0.20 for the bottom spectrum in increments of 0.20. To emphasize the effect that the variable frequencies, i.e., $\nu_j(r)$, have on the band shape, we perform the same Gaussian synthesis for *fixed* frequencies, i.e., $\nu_j=2000$, 2100, 2195, and 2265 cm^{-1} for $j=0$ to 3, respectively, and are independent of r. These frequencies have been reported in earlier reports[5-7] and were associated with the four different environments involving, respectively, three Si atoms, two Si atoms, and one O atom, etc. The results,

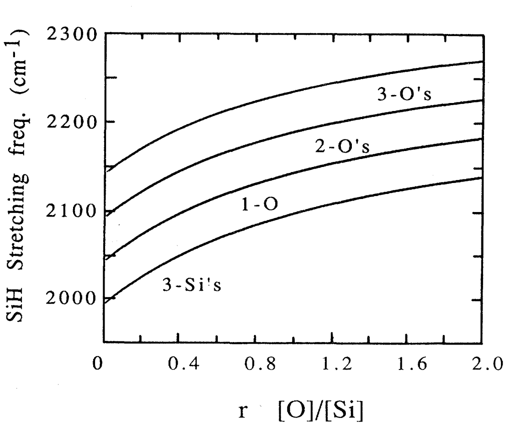

FIG. 9. SiH stretching frequency $\nu_j(r)$ for the four different local configurations vs the [O]/[Si] ratio r.

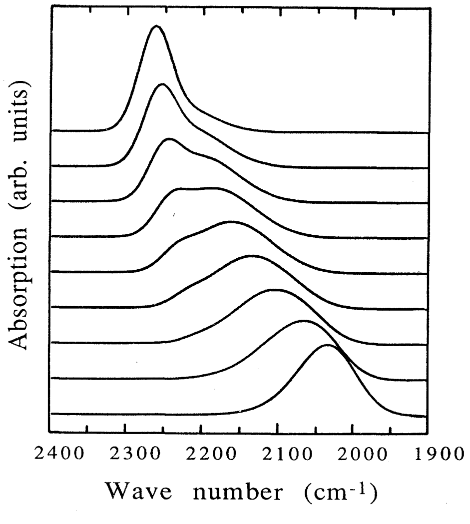

FIG. 10. Synthesis of the SiH stretching absorption band shape: the frequencies of the four subbands, $\nu_j(r)$, are determined from Fig. 9; the amplitude weighting factors $P_j(r)$ from Fig. 6; and the full width for each subband is $H_0=H_1=H_2=80$ cm^{-1}, and $H_3=50$ cm^{-1}. The [O]/[Si] ratio for the top spectrum is 1.80 and decreases, in 0.20 increments, to 0.20 for the bottom spectrum.

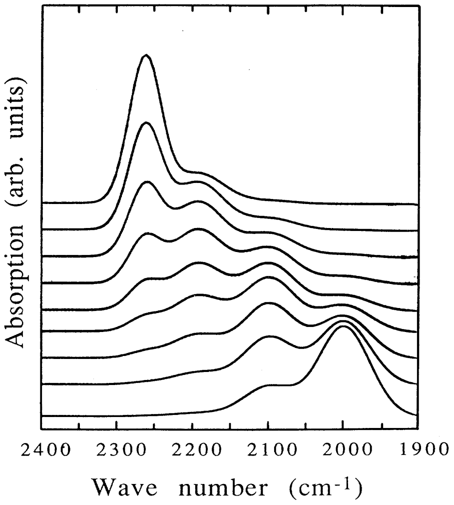

FIG. 11. Synthesis of the SiH stretching absorption band shape using fixed frequencies for each subband: $\nu_0=2000$ cm^{-1}; $\nu_1=2100$ cm^{-1}, $\nu_2=2195$ cm^{-1}, and $\nu_3=2265$ cm^{-1}. $P_j(r)$ and H_j and the range in the [O]/[Si] ratio are the same as in Fig. 10.

for the same range in r as in Fig. 10, are shown in Fig. 11. The synthesized bands shown in this figure have the same subband widths H_j and amplitudes $P_j(r)$ as those in Fig. 10. Notice that each subband is clearly identifiable in the synthesized absorption bands of Fig. 11.

V. DISCUSSION

The vibrational frequency for any coupled system can be varied in two ways: (i) by varying the force constant, or (ii) by varying the effective mode mass of the system. We have used the induction mechanism to predict how changes in the electronegativity of the neighborhood of the SiH group affect the vibrational frequency of the SiH stretching mode. Changes in the electronegativity are accomplished by replacing Si atoms with O atoms. The induction model addresses only changes in the force constant. In our analysis of the monohydride vibrations, we have neglected any changes in the mode mass because replacing the mode mass of three Si atoms by three O atoms results in a frequency shift of less than 10 cm^{-1} for the SiH stretching mode.

In synthesizing the shape of the SiH stretching band as a function of the [O]/[Si] ratio, we have used a simple statistical model of silicon suboxides to determine the relative probability that Si and/or O atoms occupy the three nearest-neighbor sites of the monohydride group. The amplitudes of the Gaussian functions representing each subband are then found from the probability functions. It is important for this analysis that the suboxide is a *homogeneous* alloy of silicon and oxygen and that the concentration of dihydride groups is small in comparison with the concentration of monohydride groups.

We have shown that for a fixed [O]/[Si] ratio the induction model predicts four distinct frequencies, one for each of the four possible HSi-$\mathrm{Si}_{3-n}\mathrm{O}_n$ environments. The induction model also predicts that for a particular local environment, i.e., for a particular value of n, the sum of the electronegativities, and therefore the vibrational frequencies, can depend on the [O]/[Si] ratio of the SiO_r network itself. We have considered two limiting cases: (1) the sum of the electronegativities depends only on the nearest neighbors, and (2) the sum depends also on the average electronegativity of the host SiO_r network which we have taken as the next-nearest neighbor. The synthesized SiH stretching-band shapes for cases (1) and (2) are shown in Figs. 11 and 10, respectively. These figures should be compared with the experimental data shown in Fig. 3. There are three features which the experimental spectra have in common with the synthesized spectra of case (2): (i) only two distinct bands are observed, (ii) the peak position of the narrow high-frequency band shows a small frequency dependence with r, between about 2270 and 2260 cm^{-1}, and (iii) the peak position of the wide low-frequency band shows a large frequency dependence, between about 2200 and 2000 cm^{-1}. The reason for the experimental loss of identity of the subbands is that, for any particular value of r, the predicted difference in frequency between any two neighboring subbands is only 50 cm^{-1}. This is less than the FWHM of the subbands themselves. We find that by including the effect of the host SiO_r network into the next-nearest-neighbor environment, a more accurate description of the SiH vibrations in silicon suboxides is obtained.

Finally, we say a few things about SiH groups in silicon nitrides and subnitrides, i.e., in SiN_r:H, where the [N]/[Si] ratio r is between 0 and 4/3. A similar type of analysis described in this paper for the suboxides can be carried out on the subnitrides. The SiH stretching frequency in SiN_r:H will depend on the relative number of N and Si nearest-neighbor atoms and on the value of r. Curves similar to those found in Fig. 9 can be calculated, assuming that the hydrogen is incorporated predominantly in the SiH groups (rather than in NH groups). The result of such a calculation is that for any particular value of r the difference in frequency between any two neighboring subbands is only half the difference in the oxides, i.e., about 24 cm^{-1}. The smaller difference is expected because nitrogen is less electronegative than oxygen. Bands separated by this amount cannot be resolved in amorphous materials because the bandwidths are typically greater than about 50 cm^{-1}. We predict that if homogeneous subnitrides can be deposited in which the hydrogen bonds only to silicon, the peak of the SiH stretching band will shift smoothly between the frequencies of the a-Si:H and a-$\mathrm{Si}_3\mathrm{N}_4$:H end points, about 2000 and 2180 cm^{-1}, respectively, with no distinct subbands developing for the [N]/[Si] ratios between 0 and 4/3. A similar behavior is expected with oxynitrides (a-$\mathrm{Si}_x\mathrm{O}_y\mathrm{N}_z$:H) containing hydrogen in the from of SiH groups if the material is a homogeneous alloy. In this case, we expect the difference in frequency between any two neighboring subbands to be between the differences found in SiO_r and SiN_r, i.e., somewhere between 50 and 24 cm^{-1}. Again, this leads to only one spectral band whose peak position depends on the alloy composition. If, on the other hand, the oxynitride is a diphasic mixture of SiO_2 and $\mathrm{SiN}_{4/3}$, at least two spectral bands can be expected.

In conclusion, we have synthesized the absorption band of the SiH stretching vibration. We have used an extended induction model which considers both the local and the remote induction effects to predict the SiH stretching frequencies in each of the HSi-$\text{Si}_{3-n}\text{O}_n$ ($n=0$ to 3) bonding configurations and find that four bands, separated by 50 cm^{-1}, are predicted. We have used a modified Philipp model of the silicon suboxide to arrive at the amplitude weighting factors. The excellent agreement between the experimental and synthesized spectra supports the assumption that was made that the SiO_r alloys are homogeneous as opposed to being diphasic mixtures of Si and SiO_2; in other words, of being composed of silicon tetrahedra of the form Si-Si_4 and Si-O_4.

ACKNOWLEDGMENTS

This research was supported by the U.S. Office of Naval Research (ONR) under Contract Nos. N00014-79-C-0133 and N00014-89-C-1057.

---

[1] M. H. Brodsky, M. Cardona, and J. J. Cuomo, Phys. Rev. B **16**, 3556 (1977).

[2] E. C. Freeman and W. Paul, Phys. Rev. B **18**, 4288 (1978).

[3] G. Lucovsky, R. J. Nemanich, and J. C. Knights, Phys. Rev. B **19**, 2064 (1979).

[4] M. A. Paesler, D. A. Anderson, E. C. Freeman, G. Moddel, and W. Paul, Phys. Rev. Lett. **41**, 1492 (1978).

[5] J. C. Knights, R. A. Street, and G. Lucovsky, J. Non-Cryst. Solids **35&36**, 279 (1980).

[6] P. John, I. M. Odeh, M. J. K. Thomas, M. J. Tricker, and J. I. B. Wilson, Phys. Status Solidi B **105**, 499 (1981).

[7] G. Lucovsky, J. Yang, S. S. Chao, J. E. Tyler, and W. Czubatyj, Phys. Rev. B **28**, 3225 (1983).

[8] C. M. Hartwig, J. Chem. Phys. **66**, 227 (1977).

[9] P. D. Richard, R. J. Markunas, G. Lucovsky, G. G. Fountain, A. N. Mansour, and D. V. Tsu, J. Vac. Sci. Technol. A **3**, 867 (1985).

[10] D. V. Tsu and G. Lucovsky, in *Plasma Processing and Synthesis of Materials,* Vol. 98 of *Materials Research Society Symposium Proceedings,* edited by D. Apelian and J. Szekely (MRS, Pittsburgh, 1987), p. 285.

[11] D. V. Tsu and G. Lucovsky, J. Non-Cryst. Solids **97&98**, 839 (1987).

[12] G. N. Parsons, D. V. Tsu, C. Wang, and G. Lucovsky, J. Vac. Sci. Technol. A **7**, 1124 (1989).

[13] P. G. Pai, S. S. Chao, Y. Takagi, and G. Lucovsky, J. Vac. Sci. Technol. A **4**, 689 (1986).

[14] D. V. Tsu, G. Lucovsky, and B. N. Davidson (unpublished).

[15] G. Lucovsky, Solid State Commun. **29**, 571 (1979).

[16] J. C. Carver, R. C. Gray, and D. M. Hercules, J. Am. Chem. Soc. **96**, 6851 (1984).

[17] D. V. Tsu, G. N. Parsons, G. Lucovsky, and M. W. Watkins, J. Vac. Sci. Technol. A **7**, 1115 (1989).

[18] D. V. Tsu, G. Lucovsky, and M. W. Watkins, in *Chemical Perspectives of Microelectronic Materials,* Vol. 131 of *Materials Research Society Symposium Proceedings,* edited by M. E. Gross, J. M. Jasinski, and J. T. Yates, Jr. (MRS, Pittsburgh, 1987), p. 289.

[19] G. Lucovsky, C. K. Wong, and W. B. Pollard, J. Non-Cryst. Solids **59&60**, 839 (1983).

[20] G. Lucovsky, M. J. Mantini, J. K. Srivastava, and E. A. Irene, J. Vac. Sci. Technol. B **5**, 530 (1987).

[21] H. R. Philipp, J. Non-Cryst. Solids **8-10**, 627 (1972).

[22] P. C. Taylor, S. G. Bishop, D. L. Mitchell, and D. Treacy, in *Amorphous and Liquid Semiconductors,* edited by J. Stuke and W. Brenig (Taylor and Francis, London, 1974).

[23] R. T. Sanderson, *Chemical Periodicity* (Reinhold, New York, 1960), pp. 16–56.